

DEFECTS ANNEALING OF Si^+ IMPLANTED GaAs AT RT AND 100°C

G. BAI, D. N. JAMIESON, M-A. NICOLET, and T. VREELAND JR.

Division of Applied Science and Engineering
California Institute of Technology
Pasadena, CA 91125

ABSTRACT

Annealing behavior of point defects near room temperature is studied by measuring the strain relaxation of Si^+ implanted GaAs. Polished semi-insulating GaAs wafers were implanted with 300keV Si^+ at liquid nitrogen (LN_2) and room temperature (RT). The strain profile was obtained by the X-ray Double Crystal Diffraction (DCD) technique and kinematical fitting. The maximum strain of the samples stored at RT and elevated temperature 100°C in air, decreases with time, which indicates the reduction of point defects. Relaxation is exponential in time. At least two time constants of 0.24hrs and 24hrs are needed to fit the data, suggesting that two different processes are responsible for annealing defects. Time constants are obtained for different doses at RT and LN_2 implantation temperature, and found to be insensitive to both these quantities. The activation energy for defect migration is estimated using simple diffusion model.

INTRODUCTION

Implantation has attracted great attention in the last decade because it has important applications in the semiconductor industry, in particular, as a technique for doping and surface modification. A great deal has been learned about ion—solid interactions, e.g., the nature of collisional cascades^[1,2,3], damage production and annealing^[4], radiation-enhanced diffusion^[5], etc. However, there are still a lot of subtle details not well understood, e.g., how post recrystallization of implanted GaAs proceeds^[6,7,8,9], which is essential for reducing defects to thermal equilibrium concentration and incorporating impurities into the lattice sites in order to have good electrical properties. In this paper, we studied the strain relaxation of Si^+ implanted GaAs at LN_2 temperature. A thorough understanding of structural changes of GaAs by radiation is crucial for doping GaAs by ion implantation. Compared to diffusion processes, doping by implantation has many advantages, e.g., well-controlled doping profiles, relatively low temperature processing, etc.

Processes which occur during implantation can be classified into two main categories^[4]:

- 1) collisional processes: atoms are displaced and Frankel pairs are generated,
 - 2) thermal processes: vacancies and interstitials recombine and migrate to their sinks.
- The final state after implantation is the result of competition between these processes. This state usually has not reached thermal equilibrium immediately after implantation, and hence is not stable at elevated temperatures. Knowledge of the time evolution of this state is both academically and technologically important. Strain is very sensitive to structural damage. Therefore, measurement of strain profile provides an easy way to study the point defect profile and its time evolution after implantation.

In this paper, we present some quantitative results about strain relaxation at RT and 100°C, of 300keV Si^+ ions implanted into GaAs at LN_2 and RT with doses from 1×10^{12} to 1×10^{15} ions/cm². Time constants are obtained by sequential measurements of the maximum strain. Two distinct time constants (differing by about two orders of magnitude) signify the existence of two different annealing processes. There exists a threshold dose, ϕ_{th} , beyond which the rocking curve flattens, indicating the dominance of amorphous zone formation over lightly damaged regions. The threshold doses (measured at RT after

implantation) are smaller for low temperature implantation ($\phi_{th} \approx 3 \times 10^{13}/\text{cm}^2$ at LN_2 implantation*) and larger for elevated temperature ($\phi_{th} \approx 1 \times 10^{15}/\text{cm}^2$ at RT implantation), due to different *in situ* annealing rates. Threshold dose also increases as the post implantation temperature increases [Fig. 2].

EXPERIMENTS AND RESULTS

Semi-insulating (100) GaAs wafers, after surface polishing and cleaning, were implanted at LN_2 and RT, with 7° beam inclination to surface normal to avoid channeling. The Si flux was kept small ($\sim 1 \mu\text{A}$) to minimize beam heating, and doses ranged from $1 \times 10^{12} \text{ Si}^+/\text{cm}^2$ (lower limit for rocking curve sensitivity) to $1 \times 10^{15} \text{ Si}^+/\text{cm}^2$ (amorphization).

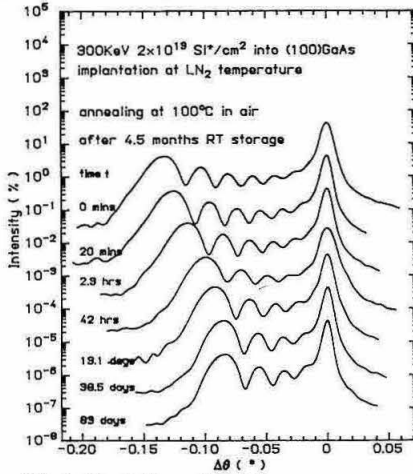


Fig.1 Evolution of rocking curves measured at RT on a (100)GaAs wafer implanted at 77K with $2 \times 10^{13} \text{ Si}^+/\text{cm}^2$, as a function of storage duration in air at RT.

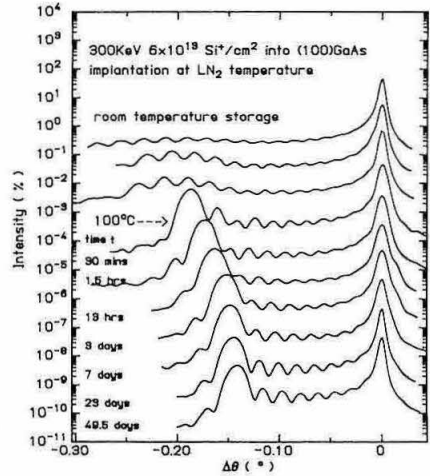


Fig.2 Evolution of rocking curves measured at RT on a (100)GaAs wafer implanted at 77K with $6 \times 10^{13} \text{ Si}^+/\text{cm}^2$, as a function of storage duration in air at RT, and subsequently at 100°C .

Strain was measured at RT by means of DCD, approximately two days after implantation, with the samples stored at RT in air. Two characteristic rocking curve patterns were obtained, corresponding to the samples of damaged single crystal [Fig. 1] and disordered structure [Fig. 2]. To get more insight into the structure of the underlying defects, channeling measurements were performed for selected samples. Again, low dose and high dose spectra have very different features [Fig. 3]. Both measurements indicate that there exists a threshold dose, $\phi_{th} \approx 3 \times 10^{13}/\text{cm}^2$, for LN_2 implantation followed by RT post annealing. At low doses ($\phi \leq 2 \times 10^{13}/\text{cm}^2$), the concentration of defects produced by irradiation is small and we have damaged single crystals. As dose increases, the number of point defects increase linearly up to the threshold dose ($\phi_{th} \approx 2 \times 10^{13}/\text{cm}^2$). Above this dose, point defect concentration is high enough to cause overlap of defects in some

* The maximum fraction of Frenkel defects corresponding to this dose was estimated to be about 10% using TRIM code, which is roughly the critical defect concentration for amorphization^[10,11].

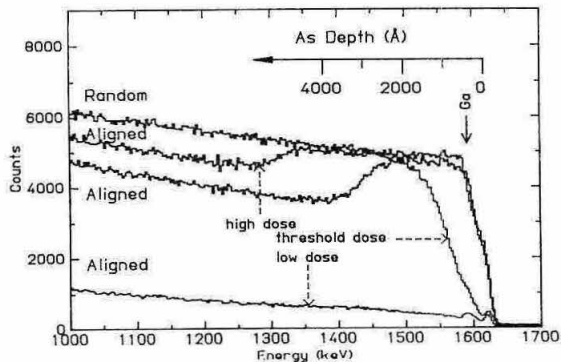


Fig.3 2 MeV ^4He backscattering and channeling spectra measured at room temperature of the samples stored in air at RT and 100°C .

regions and local disordering occurs so that an amorphous zone forms^[12,13,14]. As dose increases further, the amorphous zone grows until the entire implanted region is amorphized. Since the implantations were done at LN_2 temperature, all defects produced by collision cascades were presumably frozen during implantation^[15]. However, the measurements were done after the samples were stored at RT in air for 2 days, therefore the rocking curve gives the strain profile for the samples annealed at RT for 2 days.

The threshold dose ($\phi_{th} \approx 10^{15}/\text{cm}^2$) for RT implantation, on the other hand, is much higher than that for LN_2 (differing by approximately two orders of magnitude). This indicates the pronounced effect of *in situ* annealing. Defects recombine efficiently during implantation at RT.

In the low dose regime^[16], the maximum strain—dose relation is linear for both RT^[17] and LN_2 implantation, and in fact, basically the same [Fig. 4]. This shows that *in situ* annealing is not important in this regime because the defect concentration is very small, $< 10^{-3}$ at.%. It is interesting to note that the threshold dose for LN_2 implantation is also the onset of the linear regime for RT implantation.

Strain profiles $\epsilon^\perp(x)$ are obtained by fitting the kinematical model (valid for damaged thickness $\leq 1\mu\text{m}$) to the experimental rocking curve^[18]. It is seen

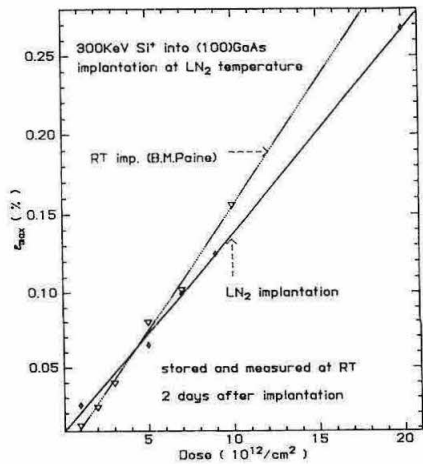


Fig.4 The relationship between the doses ϕ and the maximum perpendicular strain ϵ_{max}^\perp measured by the angular separation of substrate peak and the strongest satellite peak.

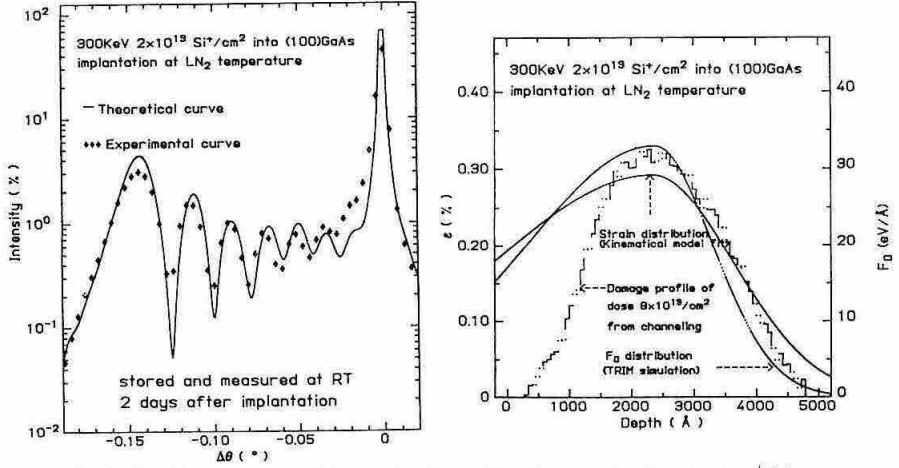


Fig.5 Rocking curves and fitted depth profile of perpendicular strain $\epsilon^{\perp}(x)$, measured at RT 2 days after implantation (100)GaAs with $2 \times 10^{13} \text{Si}^+/\text{cm}^2$ at LN_2 .

to nuclear interactions. ϵ^{\perp} and $\epsilon^{\parallel}(x)$ are not exactly proportional to each other [Fig. 5]. There are two possible explanations. We can assume that the initial strain profile is exactly proportional to $F_D(x)$ (at least for the low dose regime where $\epsilon^{\perp} \leq 0.3\%$), and the profile fitted, from measurements done two days after implantation, is due to RT annealing of point defects. Another possible explanation is that a smaller F_D is more effective at generating strain than the larger one*. To pin down this point, both a detailed understanding of the conversion mechanism of F_D to strain energy and more experimental results are needed. Strain was measured again after two months in storage at RT in air, and the rocking curves of the samples with doses less than the threshold dose were found to have changed. The maximum strain decreases. After 4.5 months, all measurements were repeated again, and strain was found to have become saturated [Fig. 1]. With all strains saturated at RT, samples were put in an oven at 100°C . Measurements were again done in time sequence. Three regimes can be identified:

(1) low dose regime: $\phi < \phi_{th}$

In this regime, there is only lightly damaged single crystal. The only change as a function of time is the decrease of strain (possibly redistribution).

(2) threshold dose regime: $\phi \approx \phi_{th}$

In this regime, a transition to damaged single crystal occurs, local disorder is annealed. After the initial transition (in a time $< 20 \text{mins}$), further annealing is similar to case (1) [Fig. 2].

(3) high dose regime: $\phi \gg \phi_{th}$

In this regime, no change was observed after annealing for several months at 100°C . This can be explained by noticing that the entire surface layer was almost amorphized in this

§ $F_D(x)$ is the energy deposition per unit length due to nuclear interactions.

* For example, if F_D is converted into strain energy u_s directly, i.e. $F_D \phi \propto u_s$, we will have $\epsilon^{\perp} \propto \sqrt{F_D}$. From linear elastic theory, we know $u_s \sim G\epsilon^{\perp 2}$, and hence $\epsilon^{\perp} \propto \sqrt{\frac{\phi F_D}{G}}$.

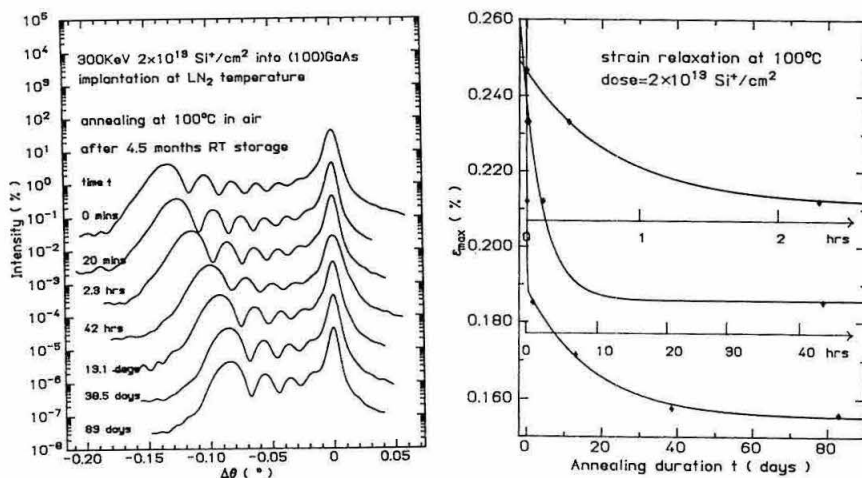


Fig.6 The decrease of the maximum perpendicular strain ϵ_{max}^{\perp} of the samples shown in Fig.2 with subsequent annealing at 100°C, measured at room temperature, as a function of storage duration at 100°C.

regime. The transition is a structural transformation (amorphous—single crystal), associated with the change of free energy of collective system. More energy is needed to activate the process, 100°C is not high enough. This is unlike the regime (2), where only local disordering is present and only individual defects or clusters annealing are associated with the transition, which can be activated with energy E_a . From sequential measurements of rocking curves, quantitative results of strain relaxation can be obtained. It is found that strain decreases exponentially with time, and at least two time constants are needed to fit the data [Fig. 6]. Two numbers are approximately 0.24 hrs and 24 hrs respectively, differing by about two orders of magnitude. Also these time constants are not sensitive to the dose and implantation temperature (time constants corresponding to the dose of $6 \times 10^{13}/\text{cm}^2$ at LN_2 implantation and $1 \times 10^{14}/\text{cm}^2$ at RT implantation are approximately the same).

DISCUSSION

It is well known that ion irradiation produces damage and *in situ* annealing has a pronounced effect of the implanted crystal. Appropriate post annealing recrystallizes the damaged layer. However, quantitative results are difficult to obtain by most methods, in particular in the low dose regime. Due to its high sensitivity to crystal strain, DCD provides a tool to study the annealing process quantitatively.

Strain relaxation at RT storage in air implies that defects are mobile near room temperature. The existence of two different time constants indicates the presence of two distinct annealing processes with different rates (differing by about two orders of magnitude).

However, rocking curve measurements only give the strain profile of damaged crystal. To relate the strain with the defect concentration of the crystal, we need to know how F_D converts to strain energy. Since the exact relation between strain and damage (i.e. F_D or

Frenkel pairs) profile is not known, we simply assume the linear relation: $\epsilon^\perp = \lambda \cdot C_D^\dagger$, ($\lambda \approx 0.01$ is the coefficient determined by the elastic properties of the material)‡. The diffusion model is then used to study the time variation of ϵ^\perp . For thermal diffusion processes with activation energy E_a , we have

$$\frac{dC_D}{dt} = -\frac{t}{\tau},$$

where the time constant is

$$\tau = \nu_r^{-1} e^{\frac{E_a}{kT}},$$

where ν_r is the vibration frequency of the atom and E_a is the activation energy of the diffusion process. In this simplest model, two different time constants correspond to two activation energies E_{a1} and E_{a2} . The difference is

$$\Delta E_a = kT \ln \frac{\tau_1}{\tau_2}.$$

With $\tau_1 \approx 0.24$ hrs and $\tau_2 \approx 24$ hrs, we obtain the difference in activation energies, $\Delta E_a \approx 1.5$ eV. We therefore conclude that to understand the physics behind strain relaxation phenomena, we need to investigate dependence of the time constants on various physical parameters such as implants, host atoms, annealing temperature, etc.

ACKNOWLEDGEMENTS

The authors wish to thank Dr. Asbeck of Rockwell International for supplying GaAs wafers. This work was supported by the NSF-Material Research Group, and monitored by Caltech.

REFERENCES

- [1] W.L.Brown, Mat.Res.Soc.Symp.Proc., 27 (1984) 53
- [2] S.Matteson, Appl. Phys. Lett., 39 (1981) 288
- [3] P.Sigmund, Appl. Phys. Lett., 25 (1974) 169
- [4] G.H.Kinchin, and R.S. Pease, Rep. Prog. Phys., 18 (1972) 1
- [5] G.J.Dienes, and A.C.Damask, J. Appl. Phys., 29 (1958) 1713
- [6] V.S.Speriosu, B.M.Paine, and M-A.Nicolet, Appl. Phys. Lett., 40 (1982) 604
- [7] K.Gamo, T.Inada, J.W.Mayer, F.H.Eisen, C.G.Rhodes, Rad. Eff., 33 (1977) 85
- [8] S.T.Picraux, Rad. Eff., 17 (1973) 261
- [9] M.G.Grimaldi, B.M.Paine, M-A.Nicolet, D.K.Sadana, J. Appl. Phys., 52 (1981) 4038
- [10] M.L.Swanson, J.R.Parsons, C.W.Hoelke, Rad. Eff. 9 (1971) 249
- [11] L.A.Christel, J.F.Gibbons, and T.W.Sigmon, J. Appl. Phys. 52 (1981) 7143
- [12] J.F.Gibbons, Proc. IEEE, 60 (1972) 1062
- [13] F.F.Morehead Jr, and B.L.Crowder, Rad. Eff. 6 (1970) 27
- [14] D.K.Sadana, Nucl. Instr. and Meth., B7/8 (1985) 375
- [15] D.V.Stevanovic, Rad. Eff. 71 (1983) 95
- [16] W.Wesch, K.Gärtner, E.Wendler, and G.Götz, Nucl. Instr. and Meth., B15 (1986) 431
- [17] B.M.Paine, N.N.Hurritz, and V.S.Speriosu, to appear in J. Appl. Phys.
- [18] V.S.Speriosu, J. Appl. Phys., 52 (1981) 6094

† C_D is Frenkel pair density, and proportional to F_D . For our experiments, $C_D^{maz} \sim 30\%$, gives $\epsilon^\perp{}^{maz} \sim 0.3\%$, which agrees with measurements.

‡ If we assume $u_s \propto F_D$, then $\epsilon^\perp = \lambda \cdot \sqrt{C_D}$.